SK00K0002

ATOMIC AND MOLECULAR PHYSICS OF PLASMA-BASED ENVIRONMENTAL TECHNOLOGIES FOR ABATEMENT OF VOLATILE ORGANIC COMPOUNDS

B. M. Penetrante, M. C. Hsiao,
J. N. Bardsley, B. T. Merritt and G. E. Vogtlin
Lawrence Livermore National Laboratory, Livermore, CA 94550

A. Kuthi
Plasma & Materials Technologies, Inc., Chatsworth, CA 91311

C. P. Burkhart and J. R. Bayless
First Point Scientific, Inc., Agoura Hills, CA 91301

ABSTRACT

Non-thermal plasma techniques represent a new generation of air emission control technology that potentially could treat large-volume emissions containing dilute concentrations of volatile organic compounds (VOCs). In order to apply non-thermal plasmas in an industrial scale, it is important to establish the electrical power requirements and byproducts of the process. There is a need for reliable data concerning the primary decomposition mechanisms and subsequent chemical kinetics associated with non-thermal plasma processing of VOCs. There are many basic atomic and molecular physics issues that are essential in evaluating the economic performance of non-thermal plasma reactors. These studies are important in understanding how the input electrical power is dissipated in the plasma and how efficiently it is converted to the production of the plasma species (radicals, ions or electrons) responsible for the decomposition of the VOCs. This paper will present results from basic experimental and theoretical studies aimed at identifying the reaction mechanisms responsible for the primary decomposition of various types of VOCs.

INTRODUCTION

Volatile organic compounds (VOCs) are emitted from manufacturing the multitude of consumer products used every day. In most manufacturing processes, either for the raw materials, intermediates, or the finished product, VOC-containing materials are present as chemicals, solvents, release agents, coatings, and decomposition products that eventually must be disposed. In such manufacturing, there is usually a large volume of gaseous effluent that contains dilute concentrations of VOCs that is vented into the atmosphere. Cost effective technologies for disposal of VOCs are being sought by government and industry.

The control of VOC emissions from dilute, large volume sources such as paint spray booths is a challenging problem. Conventional technologies, such as carbon adsorption/solvent recovery or catalytic/thermal oxidation have high annual costs per ton of VOC emissions controlled. With a large gas flow rate (85,000 to 400,000 m^3/h) and low solvent concentrations (100 ppm or less) of no possible reuse value, operating costs for conventional systems over several years can greatly exceed the installed capital cost.

In order to reduce the operating cost, novel low-temperature (ambient to 125°C) treatment technologies are being sought. The emerging technologies include low-temperature catalysts, biofiltration and non-thermal plasmas. Catalysts easily suffer from plugging, fouling or poisoning by particulates and non-VOC materials in the exhaust stream; this results in high maintenance costs [1]. The major disadvantage of biofilters is their large specific footprint, typically 5 to 25 m^2 per 1,000 m^3/h of treated gas [2]. Biofilter systems and filter materials may also require costly maintenance and replacement.

Non-thermal plasma techniques represent a new generation of air emission control technology that potentially could treat large-volume emissions containing dilute concentrations of VOCs [3]. The basic principle that these techniques have in common is to produce a plasma in which a majority of the electrical energy goes into the production of energetic electrons, rather than into gas heating. Through electron-impact dissociation and ionization of the background gas molecules, the energetic electrons produce free radicals, ions and additional electrons which, in turn, oxidize, reduce or decompose the pollutant molecules. This is in contrast to the use of plasma furnaces or torches and several chemical techniques in which the whole gas is heated in order to break up the undesired molecules.

Either electrical discharge or electron beam methods can produce non-thermal plasmas. Each of these methods can be implemented in many ways.

There are many types of electrical discharge reactors, the variants depending on the electrode configuration and electrical power supply (pulsed, AC or DC). Some of the types of electrical discharge reactors that have been investigated for VOC abatement include the pulsed corona [4-5], electrical packed bed [4], dielectric-barrier discharge [5-8], surface discharge [9], gliding arc [10] and pulsed microwave discharge [11]. Two of the more extensively investigated types of discharge reactors are based on the pulsed corona and

dielectric-barrier discharge. In the pulsed corona method, the reactor is driven by very short pulses of high voltage, thus creating short-lived discharge plasmas that consist of energetic electrons, which in turn produce the free radicals responsible for the decomposition of the undesirable molecules. In a dielectric barrier discharge reactor, one or both of the electrodes are covered with a dielectric layer, such as glass or alumina. Whereas in the pulsed corona method the transient behavior of the plasma is controlled by the applied voltage pulse, the plasma that takes place in a dielectric-barrier discharge self-extinguishes when charge build-up on the dielectric layer reduces the local electric field. Dielectric-barrier discharge reactors, also referred to as silent discharge reactors, are now routinely used to produce commercial quantities of ozone. Unfortunately, the plasma conditions suitable for the generation of ozone are not the same plasma conditions optimum for the destruction of most VOCs.

There are also many types of electron beam reactors, the variants depending on the type of cathode (e.g. thermionic or cold), electrode configuration and voltage. The electron beam method has been applied to the decomposition of a wide variety of VOCs [12-19]. In the past, the high capital cost and x-ray hazard associated with conventional MeV-type electron beam accelerators have discouraged the use of electron beam processing in many pollution control applications. Recently, however, compact low-energy (<200 keV) electron accelerators have been developed to meet the requirements of industrial applications such as crosslinking of polymer materials, curing of solvent-free coatings, and drying of printing inks. Special materials have also been developed to make the window thin and rugged. Some of these compact electron beam sources are already commercially available and could be utilized for many pollution control applications.

Whatever the type of non-thermal plasma reactor, there is a great need for reliable data concerning the primary decomposition mechanisms and subsequent chemical kinetics associated with the processing of VOCs. In order to apply non-thermal plasmas in an industrial scale, it is important to establish the electrical power requirements and byproducts of the process. There are many basic atomic and molecular physics issues that are essential in evaluating the economic performance of non-thermal plasma reactors. These studies are important in understanding how the input electrical power is dissipated in the plasma and how efficiently it is converted to the production of the plasma species (radicals, ions or electrons) responsible for the decomposition of the VOCs. This paper will present results from basic experimental and theoretical studies aimed at identifying the atomic and molecular physics responsible for the primary decomposition of various types of VOCs.

TEST FACILITY

All of our experiments were performed in a flow-through configuration. To characterize the energy consumption of the process for each

VOC, the composition of the effluent gas was recorded as a function of the input energy density. The input energy density, Joules per standard liter, is the ratio of the power (deposited into the gas) to gas flow rate at standard conditions (25°C and 1 atm). The amount of VOC was quantified using an FTIR analyzer and a gas chromatograph.

Our electron beam reactor, shown schematically in Figure 1, used a cylindrical electron gun designed to deliver a cylindrically symmetric electron beam that is projected radially inward through a 5 cm wide annular window into a 17 cm diameter flow duct. An electron beam of 125 keV energy was introduced into the reaction chamber through a 0.7 mil thick titanium window. The electron beam current was produced from a low-pressure helium plasma in an annular vacuum chamber surrounding the flow duct. This novel design facilitates highly uniform irradiation of the flowing gas. The non-thermal plasma produced by the electron beam is capable of decomposing the VOCs in polluted gas streams at high flow rates.

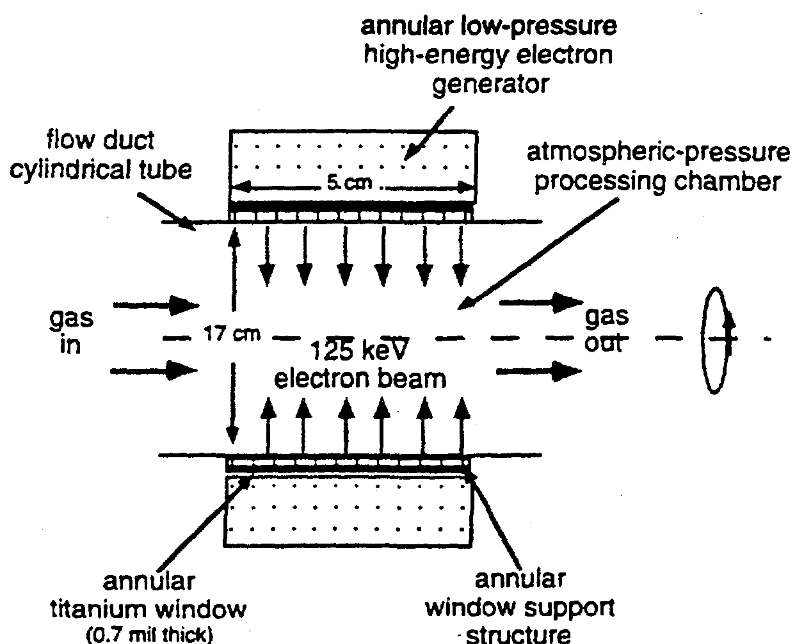

Figure 1. Schematic of the compact electron beam reactor developed by First Point Scientific, Inc. The cylindrical electron gun is designed to deliver a cylindrically-symmetric highly-uniform electron beam that is projected radially inward into the gas flow duct.

Our pulsed corona reactor is a 1.5 mm diameter wire in a 60 mm diameter metal tube 300 mm long. The power supply is a magnetic pulse compression system capable of delivering up to 15-35 kV output into 100 ns FWHM pulses at repetition rates from 15 Hz to 1.5 kHz. The power input to the processor was varied by changing either the pulse energy or pulse repetition frequency. For the same energy density input, either method produced almost identical results. The gas mixtures were set with mass flow

controllers. The gas and processor temperatures can be maintained at a temperature that can be controlled from 25°C to 300°C.

The dielectric-barrier discharge electrode structure has a similar electrode structure except that it has a dielectric material on the inside surface of the outer tube electrode. It consists of a 1.5 mm diameter wire in a 290 mm long alumina tube with inner and outer diameters of 53 mm and 58 mm, respectively. The middle 170 mm of the dielectric tube has aluminum foil coating the outside to form the other electrode.

ELECTRON AND CHEMICAL KINETICS CALCULATIONS

To calculate the ion and radical production yields by electrical discharge processing, we used the Boltzmann code ELENDIF [20] to calculate electron energy deposition. ELENDIF uses as input the specified gas composition and the electron-molecule collision cross sections. To calculate the ion and radical production yields by electron beam processing, we used the code DEGRAD [21]. DEGRAD also uses as input the specified gas composition and the electron-molecule collision cross sections. This code follows typical electrons as they perform successive collisions, and discrete energy bins are used to represent the energy degradation of an electron from a given beam energy. The procedure records the number of excitations, dissociations and ionizations, and the total number of all orders of secondary electrons. The chemical kinetics describing the subsequent interaction of the ions and radicals with the exhaust gas was studied using CHEMKIN-II [22].

RESULTS AND DISCUSSION

Carbon Tetrachloride

Figure 2 shows the results of experiments on electron beam and electrical discharge processing of 100 ppm of carbon tetrachloride (CCl_4) in dry air (20% O_2 80% N_2) at 25°C. The pulsed corona reactor requires 1277 Joules/liter for 90% decomposition of CCl_4, whereas the electron beam reactor requires only 20 Joules/liter to achieve the same level of decomposition.

Figure 3 compares the results of experiments on electron beam processing of 100 ppm of CCl_4 in dry air and humid air. Note that humidity is deleterious to the decomposition of CCl_4.

The results shown in Figures 2 and 3 bring about two questions regarding the decomposition of CCl_4. First, why is electron beam processing much more energy efficient than electrical discharge processing? Second, what is the reason for the deleterious effect of humidity on the decomposition efficiency? To answer these questions, we have to find main mechanism responsible for the decomposition of CCl_4.

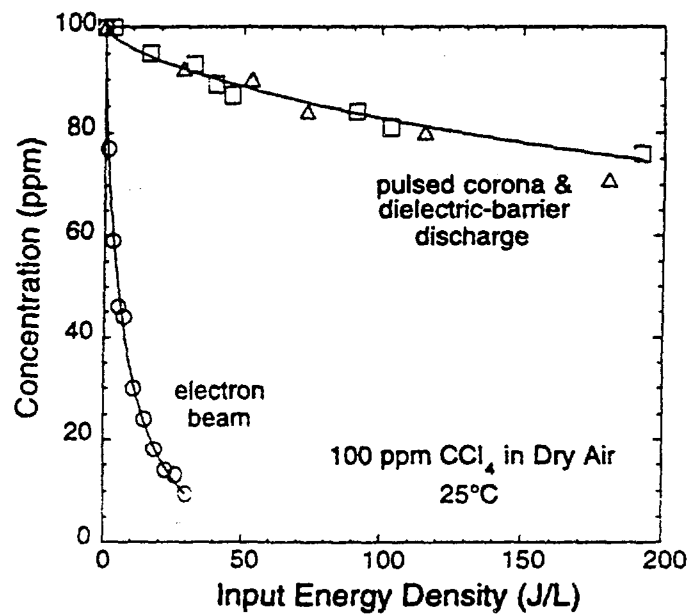

Figure 2. Comparison between electron beam and pulsed corona processing of 100 ppm of carbon tetrachloride in dry air at 25°C.

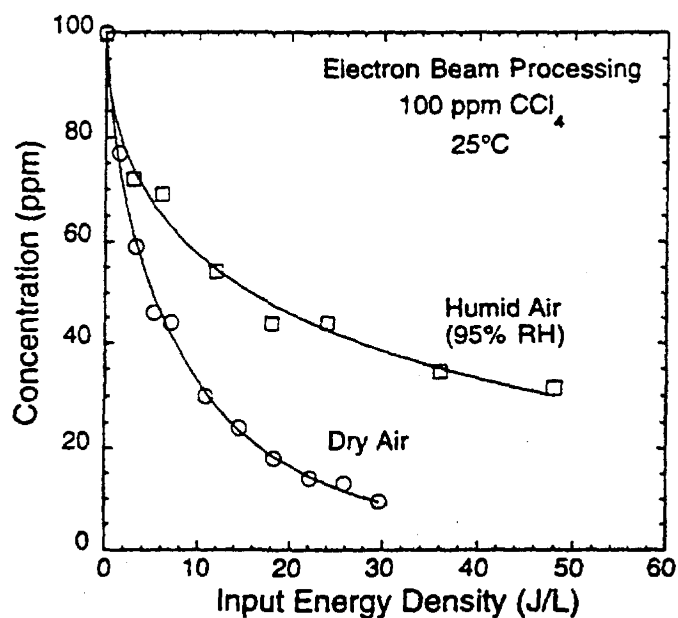

Figure 3. Electron beam processing of 100 ppm of carbon tetrachloride in dry air and humid air at 25°C.

In non-thermal plasma processing of a mixture containing very dilute concentrations of VOC molecules, the input electrical energy is dissipated by the primary electrons mostly in interactions with the background gas molecules. The energetic primary electrons produce free radicals and electron-ion pairs through electron-impact dissociation and ionization. Among the products of the primary electron-molecule reactions are atomic oxygen, $O(^3P)$ and $O(^1D)$, and atomic nitrogen, N. These radicals, as well as the secondary electrons, can subsequently react with CCl_4 and lead to its decomposition.

Table 1 shows the rate coefficients of several possible decomposition reactions. Note that the three largest rate coefficients correspond to reactions of CCl_4 with secondary electrons, $O(^1D)$, and hydroxyl radicals, OH. Because of the large concentration of O_2 in air-like mixtures, the $O(^1D)$ species are lost preferentially to quenching by O_2 (see Table 2). Any decomposition of CCl_4 via oxidation by oxygen radicals is therefore unlikely because of the very small rate coefficient for the $O(^3P)$ + CCl_4 reaction. For dry mixtures, the reaction with OH radicals is irrelevant. For humid mixtures, the OH oxidation will be significant only if the secondary electrons produced in the plasma are depleted substantially because of attachment to O_2 (see Table 2); otherwise, the CCl_4 molecules will be preferentially decomposed by dissociative electron attachment.

Table 1. Rate coefficient for carbon tetrachloride decomposition reactions. See refs. [23-28].

	REACTION	RATE COEFFICIENT (cm^3/s)	COMMENT
(1)	$O(^3P) + CCl_4 \rightarrow ClO + CCl_3$	3.2×10^{-16}	not probable
(2)	$O(^1D) + CCl_4 \rightarrow ClO + CCl_3$	3.3×10^{-10}	O(1D) lost preferentially to O_2; see reaction (6)
(3)	$N + CCl_4 \rightarrow NCl + CCl_3$	2.5×10^{-17}	not probable
(4)	$OH + CCl_4 \rightarrow HOCl + CCl_3$	1.0×10^{-12}	irrelevant for dry air
(5)	$e + CCl_4 \rightarrow Cl^- + CCl_3$	4.0×10^{-7}	most likely; competes with electron attachment to O_2; see reactions (7)-(9)

Table 2. Rate coefficients of reactions competing for electrons and O(^{1}D). Rate coefficient in units of cm^3/s for reaction (6) and cm^6/s for reactions (7)-(8).

	REACTION	RATE COEFFICIENT	COMMENT
(6)	$O(^1D) + O_2 \rightarrow O(^3P) + O_2$	4.0×10^{-11}	dominates over reaction (2)
(7)	$e + O_2 + O_2 \rightarrow O_2^- + O_2$	2.5×10^{-30}	$k_{eff} = 1.2 \times 10^{-11}$ for 20% O_2
(8)	$e + O_2 + N_2 \rightarrow O_2^- + N_2$	1.6×10^{-31}	$k_{eff} = 2.9 \times 10^{-12}$ for 75% N_2
(9)	$e + O_2 + H_2O \rightarrow O_2^- + H_2O$	1.4×10^{-29}	$k_{eff} = 1.7 \times 10^{-11}$ for 5% H_2O

An analysis of the rate coefficients shown in Table 1 suggests that the rate limiting step in the decomposition of CCl_4 is determined by the dissociative attachment of CCl_4 to the thermalized electrons in the created plasma. The specific energy consumption for CCl_4 removal is therefore determined by the specific energy consumption (or G-value) for creating electron-ion pairs.

In discharge processing, the rate coefficients for electron-impact dissociation and ionization reactions strongly depend on the electron mean energy in the discharge plasma. In pulsed corona and dielectric-barrier discharge reactors, the non-thermal plasma is produced through the formation of statistically distributed microdischarges. The electrons dissociate and ionize the background gas molecules within nanoseconds in the narrow channel formed by each microdischarge. The electron energy distribution in the plasma is complicated because the electric field is strongly non-uniform (e.g. because of strong space-charge field effects) and time dependent. However, most of the species responsible for the chemical processing are generated in the microdischarge channels already established during the main current flow. In each microdischarge column, the electrons acquire a drift velocity, v_d, and an average energy corresponding to an effective E/n, i.e., the value of the electric field E divided by the total gas density n. The efficiency for a particular electron-impact process can be expressed in terms of the G-value (number of dissociation or ionization reactions per 100 eV of input energy) defined as

$$\text{G-value} = 100\, k \,/\, (v_d\, E/n)$$

where k is the rate coefficient (cm^3/molec-s). The rate coefficient k represents the number of reactions in a unit volume per unit time. The quantity $v_d\, E/n$

represents the amount of energy expended by the electrons in a unit volume per unit time. Under most conditions encountered in pulsed corona or dielectric-barrier discharge processing, the effective E/n is close to the value for breakdown (Paschen field) [29-30]. For dry air, the effective E/n is around 130 Td (1 Td = 10^{-17} V-cm^2), which corresponds to an electron mean energy of about 4 eV.

In electron beam processing, the efficiency for a particular electron-impact process can be expressed in terms of the G-value, which is defined in the code DEGRAD as

$$\text{G-value} = 100\, N_j / E_p$$

where N_j is the number of dissociation or ionization events, and E_p is the primary electron energy.

Table 3 shows a comparison of the calculated G-values for ionization processes in dry air using an electron beam and a discharge reactor. The efficiency for production of electron-ion pairs is much higher in an electron beam reactor compared to that in an electrical discharge reactor. For electron beam processing of dry air, the ionization G-value corresponds to a specific energy consumption of 33 eV per electron-ion pair produced. For pulsed corona processing, we calculate a specific energy consumption of around 1400 eV per electron-ion pair, assuming an effective electron mean energy of 4 eV in the discharge plasma. To first order, the calculated specific energy consumption for electron-ion pair production agrees very well with our experimentally observed specific energy consumption for CCl_4 decomposition. The results shown in Figure 2 demonstrate that for VOCs requiring copious amounts of electrons for decomposition, electron beam processing is much more energy efficient than electrical discharge processing.

Table 3. Calculated G-values (number of reactions per 100 eV of input energy) for ionization processes in dry air using an electron beam and an electrical discharge reactor.

REACTION	Electron Beam	Discharge
$e + N_2 \rightarrow 2e + N(^4S, ^2D) + N^+$	0.69	$< 10^{-6}$
$e + N_2 \rightarrow 2e + N_2^+$	2.27	0.044
$e + O_2 \rightarrow 2e + O_2^+$	2.07	0.170
$e + O_2 \rightarrow 2e + O(^1D) + O^+$	1.23	0.0016

What is the probability that the electrons will attach to CCl_4 instead of oxygen? Let us first consider the case of a dry mixture. After the concentration of CCl_4 has decreased to a few tens of ppm, the three-body attachment of

thermal electrons to oxygen molecules (reactions 7 and 8 in Table 1) becomes a significant electron loss pathway compared to reaction (5). The attachment frequency of secondary electrons to O_2 in dry air at atmospheric pressure is

$$\nu_{O2} = k_{(7)} [O_2]^2 + k_{(8)} [N_2] [O_2] \approx 0.8\times10^8 \text{ s}^{-1}.$$

For 100 ppm CCl_4, the attachment frequency to CCl_4 is

$$\nu_{CCl4} = k_{(5)} [CCl_4] \approx 10^9 \text{ s}^{-1}.$$

When the concentration of CCl_4 is down to around 10 ppm, the electrons will attach to oxygen molecules as frequently as to CCl_4 molecules.

In humid air, the attachment frequency of secondary electrons to O_2 is

$$\nu_{O2} = k_{(7)} [O_2]^2 + k_{(8)} [N_2] [O_2] + k_{(9)} [H_2O] [O_2] \approx 1.5\times10^8 \text{ s}^{-1}.$$

Humidity enhances the attachment of electrons to O_2, thus effectively decreasing the efficiency for decomposition of CCl_4.

Methylene Chloride

The rate constant for dissociative electron attachment to methylene chloride (CH_2Cl_2) is five orders of magnitude lower compared to carbon tetrachloride [28]. The efficiency for producing electron-ion pairs is therefore not likely to be the key to the efficient decomposition of methylene chloride. Identification of the mechanism and plasma species responsible for methylene chloride decomposition is important for choosing the most energy efficient type of non-thermal plasma reactor.

Table 4 shows the rate coefficients of several possible decomposition reactions. Note that the three largest rate coefficients correspond to reactions of CH_2Cl_2 with nitrogen atoms, hydroxyl radicals and secondary electrons. Any decomposition of CH_2Cl_2 via oxidation by oxygen radicals is unlikely because of the very small rate coefficient.

A comparison of the rate coefficient for reaction (13) with that for reactions (7)-(9) shows that the electrons will be scavenged by electron attachment to O_2; thus, for air-like mixtures, the decomposition of CH_2Cl_2 by dissociative electron attachment is unlikely. The most likely mechanism for decomposition of CH_2Cl_2 in dry mixtures is the reaction with nitrogen atoms. For mixtures containing little or no O_2, the number of secondary electrons produced in the plasma has to be more than a factor of two greater than the number of N atoms in order for dissociative electron attachment to be the dominant decomposition mechanism for methylene chloride. For humid air mixtures, the number of OH radicals produced in the plasma has to be an order of magniture greater than the number of N atoms in order for OH oxidation to be the dominant decomposition mechanism for methylene chloride.

Table 5 shows a comparison of the calculated G-values (number of reactions per 100 eV of input energy) for dissociation processes in dry air using an electron beam and a discharge reactor. Discharge plasma conditions

are optimum for the dissociation of O_2, whereas electron beam conditions are optimum for the dissociation of N_2.

Table 4. Rate coefficient for methylene chloride decomposition reactions. See refs. [23, 28, 31-32].

	REACTION	RATE COEFFICIENT (cm^3/ s)	COMMENT
(10)	$O(^3P) + CH_2Cl_2 \rightarrow OH + CHCl_2$	6.3×10^{-16}	not probable
(11)	$N + CH_2Cl_2 \rightarrow$ products	1.5×10^{-12}	most likely
(12)	$OH + CH_2Cl_2 \rightarrow H_2O + CHCl_2$	1.6×10^{-13}	irrelevant for dry air
(13)	$e + CH_2Cl_2 \rightarrow$ products	6.5×10^{-13}	competes with electron attachment to O_2; see reactions (7)-(9)

Table 5. Calculated G-values (number of reactions per 100 eV of input energy) for ionization processes in dry air using an electron beam and an electrical discharge reactor.

REACTION	Electron Beam	Discharge
$e + N_2 \rightarrow e + N(^4S) + N(^4S,^2D,^2P)$	1.2	0.17
$e + O_2 \rightarrow e + O(^3P) + O(^3P)$	1.3	4.0
$e + O_2 \rightarrow e + O(^3P) + O(^1D)$	2.65	10.0
$e + O_2 \rightarrow O^- + O(^3P, ^1D)$	0.11	0.19

The processing of dilute concentrations of CH_2Cl_2 in N_2 provides a good starting point for determining the primary decomposition mechanism because there are only a couple of decomposition reactions that are possible. For electron beam processing in N_2, it costs 33 eV to produce an electron via electron-impact ionization and around 40 eV to produce an N atom via electron-impact dissociation. The decomposition of CH_2Cl_2 in this case will

therefore likely be dominated by reaction (11). For electrical discharge processing in N_2, it costs around 1400 eV to produce an electron via electron-impact ionization and about 240 eV to produce an N atom via electron-impact dissociation. The number of N atoms produced in an electrical discharge plasma greatly exceeds the number of secondary electrons. The decomposition of CH_2Cl_2 in this case will therefore also be dominated by reaction (11). In either electron-beam generated plasmas and electrical discharge plasmas, we therefore expect the energy consumption for decomposition of CH_2Cl_2 to be determined by the energy consumption for production of N atoms.

Figure 4 shows the results on electron beam and pulsed corona processing of 100 ppm CH_2Cl_2 in N_2. To first order, the calculated specific energy consumption for nitrogen atom production agrees very well with our experimentally observed specific energy consumption for CH_2Cl_2 decomposition.

Trichloroethylene

For the case of trichloroethylene (C_2HCl_3), the initial decomposition pathway can proceed efficiently by reactions with either electrons (in the electron beam method) or O radicals (in the electrical discharge method). Figure 5 compares electron beam and pulsed corona processing of 100 ppm C_2HCl_3 in dry air at 25°C. The energy consumption for C_2HCl_3 removal is re-

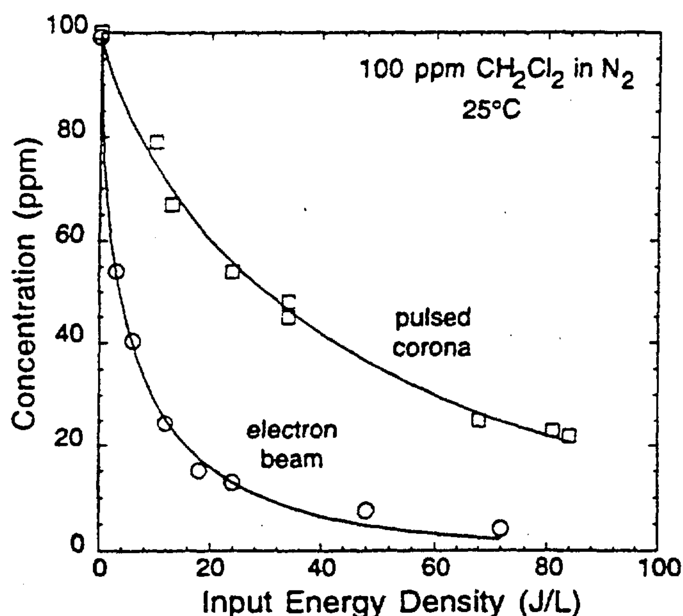

Figure 4. Electron beam and pulsed corona processing of 100 ppm methylene chloride in N_2.

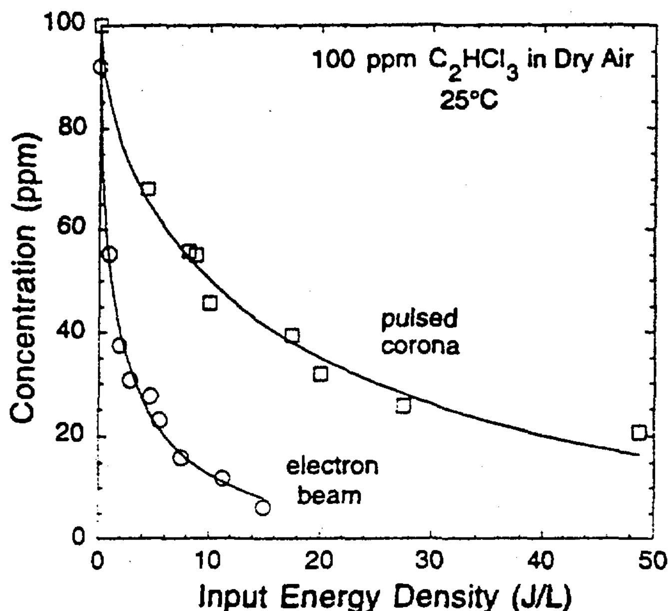

Figure 5. Electron beam and pulsed corona processing of 100 ppm trichloroethylene in dry air.

latively small using either electron beam or electrical discharge methods. This is because of a chain reaction mechanism involving chlorine (Cl) radicals. The reaction of C_2HCl_3 with electrons or O radicals initiates the detachment of Cl radicals. Other C_2HCl_3 molecules then decompose by Cl radical addition to the carbon-carbon double bond

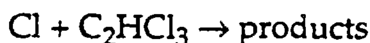

$$Cl + C_2HCl_3 \rightarrow \text{products}$$

This decomposition pathway regenerates more Cl radicals, which react with other C_2HCl_3 molecules, causing a chain reaction.

CONCLUSIONS

There is a need for reliable data concerning the primary decomposition mechanisms and subsequent chemical kinetics associated with non-thermal plasma processing of VOCs. In this paper we presented the results from basic experimental and theoretical studies aimed at identifying the reaction mechanisms responsible for the primary decomposition of three representative chlorinated VOCs, namely carbon tetrachloride, methylene chloride and trichloroethylene. The decomposition mechanisms for these compounds provide good examples of how the electron-molecule interaction physics could strongly affect the economics of the non-thermal plasma process.

[20] W. L. Morgan and B. M. Penetrante, *Comp. Phys. Comm.* **58**, 127-152 (1990).

[21] B. M. Penetrante and J. N. Bardsley, *J. Appl. Phys.* **66**, 1871-1874 (1989).

[22] R. J. Kee, F. M. Rupley and J. A. Miller, "Chemkin-II: A FORTRAN Chemical Kinetics Package for the Analysis of Gas Phase Chemical Kinetics," Sandia National Laboratories Report No. SAND89-8009B UC-706 (April 1992).

[23] J. T. Herron, *J. Phys. Chem. Ref. Data* **17**, 967 (1988).

[24] J. A. Davidson, H. I. Schiff, T. J. Brown, C. J. Howard, *J. Chem. Phys.* **69**, 4277 (1978).

[25] R. Atkinson, D. L. Baulch, R. A. Cox, R. F. Hampson, Jr., J. A. Kerr, J. Troe, *J. Phys. Chem. Ref. Data* **21**, 1125-1568 (1992).

[26] S. C. Jeoung, K. Y. Choo and S. W. Benson, *J. Phys. Chem.* **95**, 7282 (1991).

[27] A. A. Christodoulides and L. G. Christophorou, *J. Chem. Phys.* **54**, 4691 (1971).

[28] J. A. Ayala, W. E. Wentworth and E. C. M. Chen, *J. Phys. Chem.* **85**, 3989 (1981).

[29] B. Eliasson and U. Kogelschatz, *J. Phys. B: At. Mol. Phys.* **19**, 1241 (1986).

[30] B. M. Penetrante, in *Non-Thermal Plasma Techniques for Pollution Control - Part A: Overview, Fundamentals and Supporting Technologies*, B. M. Penetrante and S. E. Schultheis, Eds. (Springer-Verlag, Berlin Heidelberg, 1993) pp. 65-90.

[31] S. Miyazaki and S. Takahashi, *Memoirs Def. Acad., Jpn.* **13**, 275 (1973).

[32] N. Cohen and K. R. Westberg, *J. Phys. Chem. Ref. Data* **20**, 1211 (1991).